



This is a repository copy of *Directly coupled vs. spectator linkers on diimine Pt(II) acetylides - change the structure, keep the function?*.

White Rose Research Online URL for this paper:

<https://eprints.whiterose.ac.uk/123012/>

Version: Accepted Version

Article:

Archer, S., Keane, T. orcid.org/0000-0003-4975-0868, Delor, M. et al. (7 more authors) (2017) Directly coupled vs. spectator linkers on diimine Pt(II) acetylides - change the structure, keep the function? *Chemistry - A European Journal*, 23 (72). pp. 18239-18251. ISSN 0947-6539

<https://doi.org/10.1002/chem.201703989>

© 2017 Wiley-VCH Verlag GmbH & Co. KGaA, Weinheim. This is the peer reviewed version of the following article: Archer, S., Keane, T., Delor, M., Bevon, E., Auty, A., Chekulaev, D., Sazanovich, I., Towrie, M., Meijer, A. and Weinstein, J. (), Directly Coupled vs. Spectator Linkers on Diimine Pt(II) Acetylides - Change the Structure, Keep the Function?. *Chem. Eur. J.*, which has been published in final form at <https://doi.org/10.1002/chem.201703989>. This article may be used for non-commercial purposes in accordance with Wiley Terms and Conditions for Self-Archiving.

Reuse

Items deposited in White Rose Research Online are protected by copyright, with all rights reserved unless indicated otherwise. They may be downloaded and/or printed for private study, or other acts as permitted by national copyright laws. The publisher or other rights holders may allow further reproduction and re-use of the full text version. This is indicated by the licence information on the White Rose Research Online record for the item.

Takedown

If you consider content in White Rose Research Online to be in breach of UK law, please notify us by emailing eprints@whiterose.ac.uk including the URL of the record and the reason for the withdrawal request.



eprints@whiterose.ac.uk
<https://eprints.whiterose.ac.uk/>

CHEMISTRY

A European Journal

A Journal of



Accepted Article

Title: Directly Coupled vs. Spectator Linkers on Diimine Pt(II) Acetylides - Change the Structure, Keep the Function?

Authors: Stuart Archer, Theo Keane, Milan Delor, Elizabeth Bevon, Alexander Auty, Dimitri Chekulaev, Igor Sazanovich, Michael Towrie, Antony Meijer, and Julia Weinstein

This manuscript has been accepted after peer review and appears as an Accepted Article online prior to editing, proofing, and formal publication of the final Version of Record (VoR). This work is currently citable by using the Digital Object Identifier (DOI) given below. The VoR will be published online in Early View as soon as possible and may be different to this Accepted Article as a result of editing. Readers should obtain the VoR from the journal website shown below when it is published to ensure accuracy of information. The authors are responsible for the content of this Accepted Article.

To be cited as: *Chem. Eur. J.* 10.1002/chem.201703989

Link to VoR: <http://dx.doi.org/10.1002/chem.201703989>

Supported by
ACES

WILEY-VCH

Directly Coupled vs. Spectator Linkers on Diimine Pt(II) Acetylides – Change the Structure, Keep the Function?

Stuart A. Archer^[a], Theo Keane^[a], Milan Delor^[a,c], Elizabeth Bevon^[a], Alexander J. Auty^[a], Dimitri Chekulaev^[a], Igor V. Sazanovich,^[a,b] Michael Towrie,^[b] Anthony J. H. M. Meijer,^{*[a]} and Julia A. Weinstein^{*[a,d]}

Abstract: Modification of light-harvesting units with anchoring groups for surface attachment often compromises light-harnessing properties. Here, a series of [Donor-Acceptor-Anchor] Platinum(II) diimine (bis)acetylides has been developed in order to systematically compare the effect of conjugated vs. electronically decoupled modes of attachment of protected anchoring groups on the photophysical properties of light-harvesting units. The first examples of “decoupled” phosphonate-diimine Pt(II) complexes are reported here, and their properties compared and contrasted to those of carboxylate analogs studied by a diversity of methods. Ultrafast TRIR and transient absorption spectroscopy revealed that all complexes possess a charge transfer lowest excited state, with life-times between 2 and 14 ns. Vibrational signatures and dynamics of charge-transfer (CT) states have been identified; with the assignment of electronic states and their vibrational origin aided by TDDFT calculations. Ultrafast energy re-distribution accompanied by structural changes was directly captured in the CT states. A significant difference between the structures of the electronic ground and charge-transfer excited states, as well as the differences in the structural reorganisation in the complexes bearing directly attached vs. electronically decoupled anchoring groups, has been discovered. This work demonstrates that decoupling of the anchoring group from the light-harvesting core via a saturated spacer is an easy approach to combine surface attachment with high reduction potential and 10-fold longer lifetime of the charge-transfer excited state of the light-absorbing unit, and retain electron transfer photoreactivity essential for light-harvesting applications.

Introduction

Platinum diimine/triimine-based photosensitisers for dye sensitised solar cells and for photocatalytic applications have received a great deal of attention in the last two decades[1–4], albeit far less than their d⁶ counterparts. However, for transition

metal complexes to be used in most solar powered devices, they must first be coupled, covalently or otherwise, to an interface through which external redox reactions can be driven. Whilst several strategies to such attachments exist, one of the most commonly employed is the anchoring of transition metal complexes to semiconductors – such as TiO₂, ZnO, Nb₂O₅, Ta₂O₅, or doped SnO₂,[5] which are capable of storing multiple redox equivalents. This is an essential requirement if multi-electron redox reactions, such as the splitting of water, are to be catalysed. Such “dyes” for photosensitising applications require a functional group to anchor them on to the semiconductor surface. The most typical anchoring groups are carboxylates, or rather less frequently used phosphonates.[6,7] However, phosphonate anchoring groups have shown a greater affinity to semiconductor surfaces, and chemical stability of the anchor-semiconductor bond whilst anchoring to TiO₂ surfaces,[6] demonstrated for instance, for Ru(II) bipyridyl (bipy) complexes in aqueous media at pH 3–11 [8].

An important consideration is whether the anchoring group is attached directly to the diimine or whether an “insulating” spacer group is introduced.[6,7,9–11] whereby permitting anchoring without altering the properties of the original compound. A recent comprehensive study of Ru(II) and Re(I) photosensitisers reported that introduction of a methylene spacer between the phosphonate anchoring group and the diimine considerably increases the rate of photoinduced electron injection into the semiconductor from the photosensitiser[12], the effect that may be partially attributed to the differences in the energies of the diimine-based LUMO.

The readily tunable optical and electrochemical properties of Pt(II) charge transfer complexes^[2] render these chromophores promising candidates as photosensitizers for solar energy conversion.[13–19] The first example of such a system was a dye-sensitised solar cell containing a Pt(II) carboxylate dye, reported in 2000^[13], which utilised a quinoline dithiolate donor ligand attached to a Pt(II) centre with dicarboxyl bipyridine /phenanthroline acceptor ligands. The (dicarboxy-bipyridine)Pt(quinolone-dithiolate) complex achieved a solar energy conversion efficiency of 2.6% and an open-circuit potential of 600 mV under AM 1.5 solar irradiation. Several further studies concentrated on Pt(II) maleonitrile dithiolate (mnt) based dyes^[15,16], where the effect of the position of the carboxylate spacer on the solar conversion efficiency was investigated; the 3,3'-isomer was found to be most effective, with efficiencies of ~3.6%. Pt(diimine)(catecholates) have also been integrated into DSSCs through a carboxylate spacer, with the overall efficiencies between 0.02–0.07%, attributable to the short lived excited state of this class of molecules (~250 ps)^[20].

Pt(II) bipy acetylide complexes, which intensely absorb across the visible range of the spectrum, have been well studied^[1,2,4,21–24]

[a] Dr. S. A. Archer, Dr. M. Delor, E. Bevon, Dr. T. Keane, Dr. I. Sazanovich, Dr. A. Meijer, Prof. J.A. Weinstein
Department of Chemistry, University of Sheffield
Brook Hill, Sheffield, S3 7HF, UK
Fax: (+) 44 (0)114 222 9346
E-mail: Julia.weinstein@sheffield.ac.uk

[b] Dr. I. Sazanovich (present address), Prof. M. Towrie
Central Laser Facility, Research Complex at Harwell
Science and Technology Facilities Council, Rutherford Appleton
Laboratory, Didcot, Oxfordshire, OX11 0QX, UK

[c] Dr. M. Delor (present address), University of California Berkeley,
Berkeley, CA94720, United States of America

[d] Department of Chemistry, Moscow Lomonosov State University,
Russia

Supporting information for this article is available on the WWW under <http://www.chemeurj.org/> or from the authors.

FULL PAPER

with regard to their photophysical properties, yet there are surprisingly few examples reported of these type of complexes as photosensitisers.^[19,25] A series of Pt(II) bipy-acetylide dyes anchored via carboxylate linkers onto thin-film nanocrystalline TiO₂ has been used in DSSC^[19]. Pt(bipy)acetylide attached to TiO₂ via a directly coupled phosphonate group has been used in light-driven generation of H₂ from aqueous protons^[25].

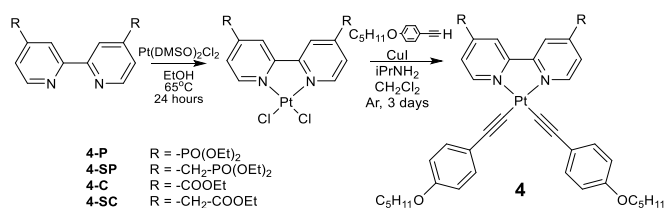
Here, Pt(II) bipy acetylide complexes bearing phosphonate ester groups, either attached directly to the bipy ligand or via a –CH₂– spacer, are presented along with their carboxylate ester counterparts. The 4-ethynylpentylbenzene acetylide ligand has been chosen as these types of Pt(II) bipy complexes demonstrate significantly longer excited state lifetimes when compared with thiolate or catecholate systems, as the strong ligand field of the acetylide carbanion raises the energy of metal centered *d-d* states which may provide a pathway for non-radiative decay of the excited state^[1,4,26]. The photophysical properties of the complexes bearing carboxylate vs. phosphonate groups, and of the directly conjugated vs. decoupled modes of attachment will be examined; the discussion on electronic structure and properties is supported by DFT calculations.

The anchoring groups employed are also strong IR reporters, permitting the use of time-resolved infrared spectroscopy, TRIR, to elucidate the nature and dynamics of the excited state(s) involved, and the potential structural and dynamic differences between the studied compounds, thus evaluating their potential in light-harvesting applications.

Results and Discussion

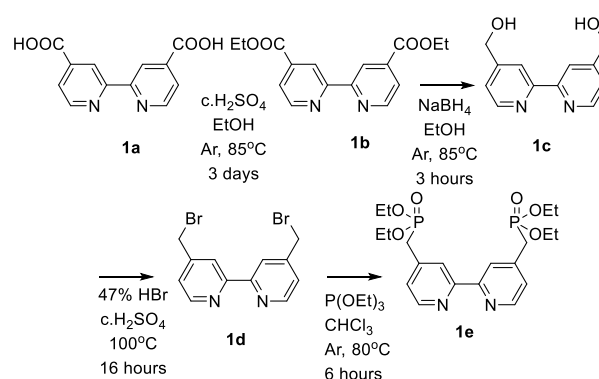
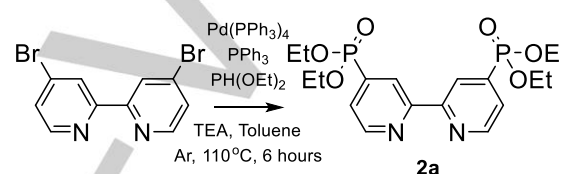
Synthesis and Characterisation

Four platinum (II) bipy acetylide complexes (Scheme 1, compounds **4-P**, **4-SP**, **4-C**, **4-SC**) have been synthesized, with variations in the type of anchor present at the 4,4' positions and the presence or absence of a methylene spacer between the bipy rings and the anchoring group.

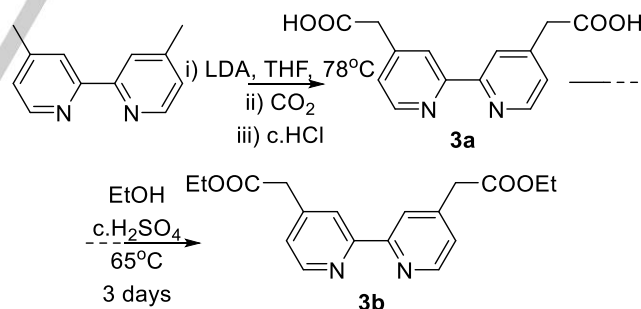


Scheme 1. Synthesis of platinum acetylide complexes.

Ligands **1b** and **1e** were synthesized according to a modified literature procedure^[6] (Scheme 2). It was found that following the ratios of reagents and solvents for the borohydride reduction of **1b** to **1c** resulted in the formation of a gel-like layer on the surface of the reaction mixture and substantial reduction in yield. This effect was countered by increasing the quantity of ethanol from 50 ml to 75 ml during the reaction, which hindered the formation of the gel layer and resulted in a yield of 50%.

Scheme 2. Synthesis of Ligands **1b** and **1e**Scheme 3. Synthesis of ligand **2a**.

Ligand **2a** was also synthesized according to a modified literature procedure^[11] (Scheme 3). It was found that, in our hands, the use of 2% methanol in chloroform rather than the reported 1% methanol in dichloromethane as the chromatographic eluent resulted in greater separation on both the TLC plates and during subsequent column chromatography purification. All of the final bipy ligands were isolated as pale pink solids.

Scheme 4. Synthesis of ligand **3b**.

Ligand **3b** was synthesized by the esterification of the acid precursor **3a**, which had been prepared according to a modified literature procedure^[27] (Scheme 4). The final step of the published procedure was the protonation of the lithium salt precursor of **3a** with HCl to produce the desired product as a precipitate, however this step did not lead to a precipitate in our hands, as the diacid product was found to be remarkably water soluble between pH 1–12. Therefore, following the reaction with CO₂, the solvent was removed from the reaction mixture under vacuum and the residue dissolved in the minimum volume of H₂O. This was washed with

FULL PAPER

dichloromethane to remove any unreacted starting material prior to acidification with 37% HCl to approximately pH 2. The water was removed under high vacuum and the resulting solid used in the esterification without any further purification.

Pt(II) complexes **4-P**, **4-SP**, **4-C** and **4-SC** were synthesized by initial reaction of the appropriate bipy ligand with Pt(DMSO)₂Cl₂, followed by the Cu(I) iodide catalysed coupling of 4-ethynylpentoxybenzene to the resultant intermediate (Scheme 1). After silica-gel purification, complexes **4-P** (99%) and **4-C** (78%) appeared as dark red solids, **4-SP** (88%) and **4-SC** (65%) as bright orange solids.

Upon complexation of the bipy, all Pt(II) compounds show ¹H NMR spectra similar to that of the free bipy ligands. The protons at the 5 and 6 positions are shifted downfield, whereas the proton at the 3 position shifts upfield slightly. The proton at position 6 shows significant broadening due to coupling with the I = 1/2 ¹⁹⁵Pt nuclei. The two methylene protons on the spacer for complex **4-SP** appears as a doublet with J = 22 Hz due to coupling with the ³¹P nucleus on the phosphonate ester. The ³¹P NMR proton-decoupled spectra show singlet resonances at 11.92 and 21.92 ppm for **4-P** and **4-SP** respectively. The significant downfield shift of **4-SP** is attributed to the greater distance of the phosphorous nuclei from the shielding effect of the π-system on the bipy ring.

In order for these complexes to effectively anchor onto a semiconductor surface, the respective ester must be hydrolysed to their acid precursors. Carboxylate esters hydrolysis is typically either acid or base catalysed in the presence of water^[28]. Historically, due to their biological significance, phosphonate esters have been extensively hydrolysed using enzymes under mild conditions^[29–31], however they also hydrolyse under acidic or basic conditions in a similar manner to carboxylate esters^[32]. For the complexes detailed here, acid hydrolysis is not possible due to the presence of the acid-sensitive acetylide ligands and Pt-C bond, necessitating acid-free hydrolysis conditions. The details of the three methods attempted here, utilizing TMSBr, KOH and NaOTMS, although none of the methods yielded pure products, are included in the supporting information.

Electronic Absorption Spectroscopy

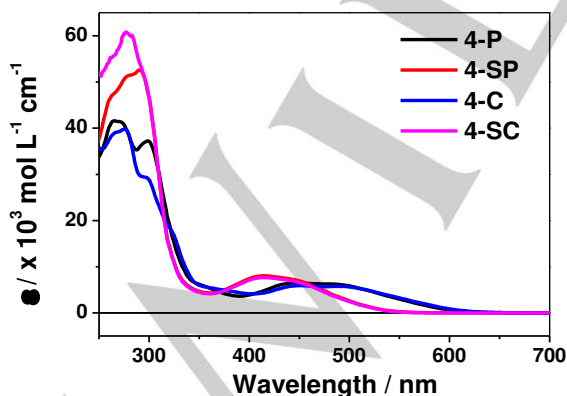


Figure 1 Absorption spectra of Pt(II) complexes recorded in dichloromethane at room temperature.

The electronic absorption spectra of all complexes were measured in dichloromethane at room temperature (Figure 1 and Table 1). The two pairs of complexes (with or without methylene spacers) exhibit very similar absorption properties. The higher energy electronic absorption bands between 250–350 nm are assigned to intraligand π–π* transitions. In the visible region, **4-SP** and **4-SC** exhibit a broad band at approximately 450 nm, whilst removal of the spacers in **4-P** and **4-C** shifts the band to lower energy, at approximately 500 nm, with the appearance of both sets of bands suggesting that at least two transitions occur in this region.

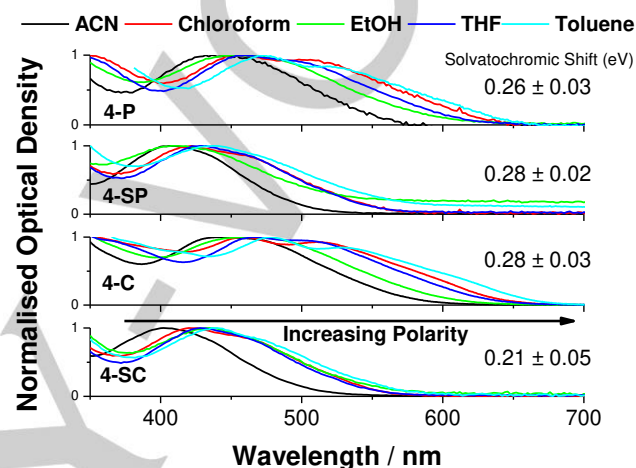


Figure 2 Solvatochromism of the lowest energy absorption band in the studied compounds at r. t. Solvatochromic shift value calculated using the method from ref. ^[33] are shown on the right; with the corresponding data in the SI.

This blue shift in the absorption maximum is consistent with a metal-to-ligand/ligand-to-ligand charge transfer (ML/LL'CT) type transition, where there is significant involvement of the bipy π-system in the LUMO^[1,26,34–38]. The effect of the methylene spacer is to decrease the electron-withdrawing effect of the carboxyl-/phosphonic ester group, thus destabilizing the LUMO, increasing the HOMO-LUMO energy gap and consequently the energy of the corresponding absorption band. This is confirmed by the calculations, which show an increase in the band gap in **4-P** vs. **4-SP**, and **4-C** vs. **4-SC** upon inclusion of the spacer (*vide infra*).

The extinction coefficients (ε, Table 1) for complexes **4-SP** and **4-SC** are nearly identical (7950 ± 50 L mol⁻¹cm⁻¹). The ε values for complexes **4-P** and **4-C** are also very similar, consistent with previous studies between the acid derivatives of these esters in the absence of a methylene spacer, whereby no significant change in absorption between the phosphonate and carboxylate was observed^[6,7,12,39]. This supports the argument that the methylene spacer decouples interactions between the anchor and the ring, with no significant differences observed in light absorption properties between the carboxylate or phosphonate.

The transitions observed in the visible region for all complexes exhibit negative solvatochromism (Figure 2) typical for MLCT/LLCT transitions, i.e. the transition λ_{max} shifts to longer

FULL PAPER

wavelengths with decreased solvent polarity. This solvatochromic shift is consistent with a charge transfer type transition. An empirical scale to determine the relative degree of solvatochromism was devised by Cummings et al^[33], based upon the relative polarities of common organic solvents using the complex Pt(bis(t-butyl)bipyridine)toluene dithiolate. This method may be applied to the complexes discussed here, as the orbital basis for the transitions observed here are very similar to that of the Pt(diimine)(dithiolate) complexes i.e. MMLL'CT. The calculated gradient from a plot of transition energy against solvent parameter gives the solvatochromic shift parameter, allowing for a numerical comparison of the strength of the solvatochromic effect (Figure S1).

All complexes show good agreement with this method, with a similar degree of solvatochromic shift for all of the complexes investigated, implying a similar relative change in dipole between the ground and excited state^[40,41]. No significant variations were observed for complexes with or without a methylene spacer. The values obtained are comparable with those previously reported for Pt(diimine)(dithiolate) complexes which possess similar charge transfer transitions^[33,42-44].

Time-dependent density functional theory (TD-DFT) calculations were performed to help resolve the electronic absorption spectra of the compounds **4**. The full details of these calculations can be found in the SI. TD-DFT has been employed to assign electronic spectra for transition metal complexes.^[45,46] The calculated transitions in the visible region correspond to a mixed metal-to-ligand/ligand-to-ligand charge transfer (ML/LLCT) type, where the shift of electron density occur from the acetylide-centred occupied orbitals to the bipy-centred unoccupied orbitals, with some minor Pt d-orbital contributions.

Electrochemistry

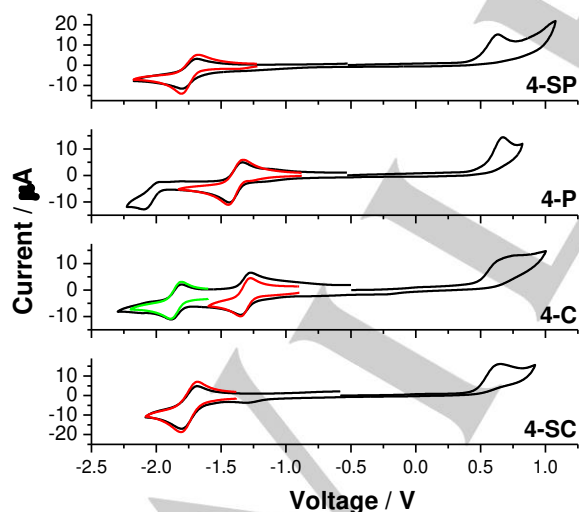


Figure 3. Cyclic voltammetry of all complexes was performed in ca. 1mM solutions in dichloromethane containing 0.2 M TBAPF₆ at room temperature, and are reported vs. Fc/Fc⁺ internal standard. The red and green traces show the isolated 1st and 2nd reduction processes scanned. All scans shown were recorded at 100 mV s⁻¹ scan rate.

The electrochemical behavior of all complexes was analysed by cyclic voltammetry performed on 1mM solutions of the complexes in dichloromethane containing 0.2M TBAPF₆ (Figure 3). The potential was measured against a 3M Ag/AgCl reference electrode with a Pt-wire counter electrode and reported against the Fc/Fc⁺ couple, which was measured concurrently. A glassy carbon working electrode was employed for the study of all complexes but **4-SC** for which a Pt disc electrode was found to be more suitable.

All complexes displayed an electrochemically irreversible oxidation process between 0.67-0.73 V, attributed to the oxidation of the platinum-acetylide subunit. The position and irreversible nature of this oxidation process is typical for platinum-bipy-acetylide complexes of this type^[26,34,36,38,47,48]. Little variation in oxidation potential between the four complexes implies that, as expected, the bipy ligands have little involvement.

Complexes **4-SP** and **4-SC** exhibit a reversible one-electron reduction process at -1.63 V and -1.75 V respectively, which is the value similar to that of E^{1/2}_{red} of (4,4'-diMe-bipy)Pt(acetylide)₂, confirming that electronic properties of **4-SP** and **4-SC** are unaffected by the anchoring group. **4-P** and **4-C** show similar reductions at significantly less negative potentials, -1.39 V and -1.31 V, resp. A second one-electron reduction was observed for **4-C** at -1.84 V; the potential difference of 0.53 V between the first and second reduction processes is typical for electron pairing energy in the same bipy-based orbital in Pt(II) polypyridine complexes,^[15, 18] suggesting that both reductions involve the same bipy orbital in **4-C**. A second reduction is also detectable for **4-P** at approx. -2 V, however it occurs in the solvent breakdown region and could not be characterized fully.

Generally, the complexes containing a methylene spacer show a more negative reduction potential than those without. This is consistent with the LUMO being destabilized with the less electron withdrawing groups, which follows from the absorption data presented above. The data also confirm that the LUMO is largely localized on the bipyridine, as is the case with similar complexes,^[19,21,24,25] the notion also confirmed by the DFT calculations (Figure 4).

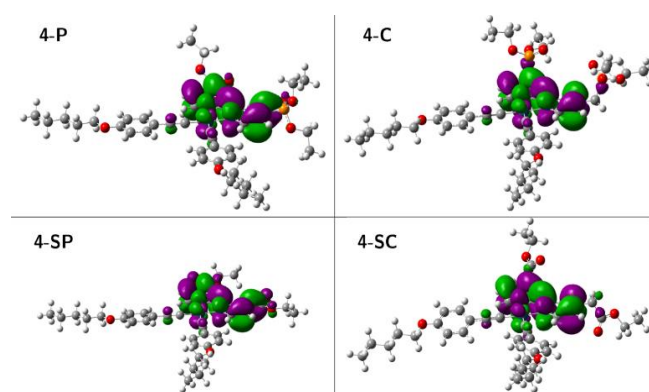


Figure 4 LUMOs of compounds **4-C**, **4-SC**, **4-P** and **4-SP** calculated in dichloromethane at the B3LYP/SDD+6-311G(d,p) level of theory. The LUMOs of **4-C** and **4-P** have some electron density present on the heteroatoms of the ester and phosphate ester respectively, which does not occur in the case of **4-SC** or **4-SP**.

FULL PAPER

Table 1 - Summary of photophysical and electrochemical properties of complexes **4-P**, **4-SP**, **4-C** and **4-SC**.

Complex	$\lambda_{\text{abs}}^a / \text{nm}$ ($\epsilon / \text{L mol}^{-1} \text{cm}^{-1}$)	Emission		TRIR		TA	$E^{p,a} / \text{V}^d$	$E^{1/2}_{\text{red}} / \text{V}$	$\Delta E_{(\text{ox-red})} / \text{V}$	
		$\lambda_{\text{em}} / \text{nm}^b$ (ϕ)	τ (em) / ns ^b	τ_1 / ps^c	τ_2 / ns^c	τ / ns				
4-P	446 (6550 ± 50)	RT	~700 (<0.002)	~ 2	19 ± 2	2.0 ± 0.2	1.9 ± 0.5	0.70 (irr.)	-1.39	2.09
		77K	620	1450 ± 150 (90%) 250 ± 30 (10%)						
4-C	450 (6680 ± 50)	RT	~710 (<0.002)	< 2	18 ± 2	1.7 ± 0.2	1.9 ± 0.5	0.73 (irr.)	-1.31 -1.84	2.04
		77K	625	2100 ± 100 (33%) 800 ± 100 (67%)						
4-SP	416 (7950 ± 50)	RT	665 (0.01)	14 ± 2	11 ± 2	> 6 ^e	11 ± 2	0.69 (irr.)	-1.63	2.32
		77K	550	3400 ± 50 (80%) 1400 ± 100 (20%)						
4-SC	412 (7950 ± 50)	RT	640 (0.02)	13 ± 2	14 ± 2	> 6 ^e	12 ± 2	0.67 (irr.)	-1.75	2.42
		77K	535	2450 ± 200 (66%) 1100 ± 100 (34%)						

^a in dichloromethane. ^b from room temperature spectra in dichloromethane, 77 K spectra in 2-methyltetrahydrofuran. Quantum yield calculated relative to aqueous [Ru(bipy)₃]Cl₂·6H₂O. Emission decay is multiexponential due to typical aggregation effects upon cooling, and is approximated by two exponential decay; individual numbers can not be considered as two distinct lifetimes. ^c in d₂-dichloromethane, calculated from major transient bands across 1350-1800 cm⁻¹. ^d vs. Fc/Fc⁺, 1 mM complex in dichloromethane containing 0.2M TBAPF₆. ^e anodic/cathodic peak separation for the Fc⁺/Fc couple used as the internal standard was 0.08 V. ^f Value approximated from data collected up to instrument-limited delay of 2500 ps.

Emission Spectroscopy

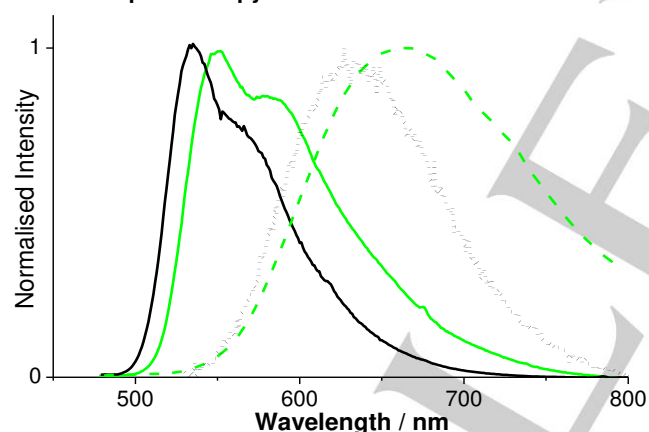


Figure 5. Normalised room temperature (---) in dichloromethane, and 77K (solid line) emission spectra for **4-SP** (black) and **4-SC** (green) obtained in 2-Me-THF. Spectra of **4-P** and **4-S** are given in the SI.

The emission spectra (Figure 5) and lifetimes of all complexes were measured at room temperature in degassed dichloromethane and also at 77K in optically transparent glass of 2-Methyltetrahydrofuran (Me-THF), under excitation in the charge transfer absorption band.

All complexes displayed broad, structureless emission band at room temperature centered at 660 – 750 nm, which is comparable with that of similar platinum-acetylide complexes^[2]. The large difference between absorption and emission maxima

supports the assignment of the lowest excited state as a triplet state (typical for Pt(II) acetylides). Emission lifetime for **4-SP** and **4-SC** in aerated DCM solution ($\tau_{\text{em}} = 14$ and 13 ns respectively) are comparatively long for NIR emitters. No increase in emission lifetime was observed upon deoxygenating the solutions. Quantum yields of 0.011 (**4-SP**) and 0.016 (**4-SC**) are consistent with related complexes^[36]. It was not possible to determine the lifetime of the excited states in **4-C** and **4-P** from the emission data because the weak emission signal ($\phi < 0.002$) was convoluted with the instrument response function. Instead, excited state lifetime was determined from transient infrared data discussed below. The fact that **4-SP** and **4-SC** show higher emission energies and quantum yield, and lifetimes compared with **4-C** and **4-P** is consistent with the energy gap law.^[49]

All complexes are emissive at 77K, with the emission maxima at significantly higher energy when compared to the room temperature spectra, a rigidochromic effect typical for emission emanating from a CT excited state. Vibronic progression features can be observed for each complex, with an energy spacing of approximately 1200 cm⁻¹, which can be assigned to the vibrational modes of the bipyridine skeleton.^[4,19,36,49] The excitation spectra for all complexes closely match their corresponding electronic absorption spectra. The non-exponential emission decay observed at 77 K can be attributed to emission from individual molecules and aggregates which are typical for square-planar Pt(II) complexes in frozen solutions; this decay has been approximated satisfactorily by two decay constants, but those cannot be attributed to individual emissive states, or species.

The trend in the emission properties of the compounds is generally in agreement with the results discussed above. The emission maxima for complexes with the methylene spacer occur

FULL PAPER

at higher energies than of those without the spacer ($\sim 2000\text{ cm}^{-1}$ shift at 77 K). For complexes **4-SP** and **4-SC**, emission from the phosphonate complex occurs at slightly lower energy with respect to the carboxylate ($\sim 600\text{ cm}^{-1}$), consistently with a slightly greater electron withdrawing effect of the phosphonate group. This is mirrored by the electrochemical data where the first reduction of **4-SP** occurs 120 mV lower than that of **4-SC**. For **4-C** and **4-P**, the effect is reversed with the phosphonate complex occurring at slightly higher energy, however the actual difference between the complexes is much smaller ($\sim 150\text{ cm}^{-1}$).

Fourier Transform Infrared Spectroscopy (FTIR)

FTIR spectra (Figure 6) of all four complexes share a number of similar spectral features. All possess a band at 2116 cm^{-1} , with a slight shoulder at higher energy, associated with the antisymmetric and symmetric combinations of the acetylide stretching modes, $\nu(\text{C}\equiv\text{C})$. In the fingerprint region of the spectrum of all four complexes, a typical $\nu(\text{C}=\text{N})$ stretching mode of the bipy ligand at 1603 cm^{-1} is present. However, for **4-SC** and **4-SP**, an additional band appears at $\sim 25\text{ cm}^{-1}$ lower energy; similar splitting was observed in the FTIR spectra of the corresponding $\text{Pt}(\text{bipy})\text{Cl}_2$ precursors, but not observed in the FTIR spectrum of the uncomplexed bipy ligands.

The FTIR spectra of both **4-C** and **4-SC** contain a band corresponding to the $\nu(\text{C}=\text{O})$ stretch at 1731 and 1735 cm^{-1} respectively. In **4-P** and **4-SP**, the $\text{P}=\text{O}$ ($1250\text{--}1299\text{ cm}^{-1}$ for phosphate esters) and $\text{P}-\text{O}-\text{C}$ (aliphatic: $970\text{--}1050\text{ cm}^{-1}$ aromatic: $1160\text{--}1260\text{ cm}^{-1}$) stretching vibrations^[50] overlap with those expected for vibrations associated with the bipy ligand.

Density functional theory (DFT) calculations were performed to assign the vibrational spectra of compounds **4**. It was found that 8 aromatic 'breathing' vibrational modes, involving the bipy-type ligands and the 4-ethynylpentylbenzene acetylide ligands, were responsible for the IR absorption bands between 1530 and 1650 cm^{-1} . The inclusion of a CH_2 spacer in the anchoring group alters the nature of the bipy-centred vibrational modes. All compounds **4** exhibited breathing modes centred on the aromatic rings of the acetylide ligands coupled with scissoring modes of the pentyl substituents at approximately 1500 cm^{-1} , corresponding to experimentally observed bands in this region. **4-P** and **4-SP** both displayed $\nu(\text{P}=\text{O})$ modes calculated at approximately 1240 cm^{-1} , slightly outside the expected region ($1250\text{--}1299\text{ cm}^{-1}$ for phosphate esters^[50]). An intense breathing mode centred on the aromatic rings of the acetylide ligands is coupled with wagging modes of the pentyl substituents, at approximately 1235 cm^{-1} , suggesting resolution of these modes in the experimental spectra may be difficult. Compounds **4-P** and **4-SP** also both displayed $\nu(\text{P}-\text{O}-\text{C})$ modes, coupled with bipy-centred aromatic breathing modes, at approximately 1025 cm^{-1} . The results of these calculations are discussed in full in the SI.

Ultrafast Time-Resolved Infrared Spectroscopy

Excited state dynamics and the influence of the nature of the spacer have been investigated by both TRIR and transient absorption spectroscopies. Promotion to the excited state with a

400 nm , $\sim 50\text{ fs}$ laser pulse leads to drastic changes in the IR spectra. In all cases (Figure 6), a bleach of the ground state bipy/Pt localised stretching vibrations at $\sim 1600\text{ cm}^{-1}$ is accompanied by the formation of a strong transient band between $1565\text{--}1580\text{ cm}^{-1}$. The broad transient bands at early times are associated with the initially formed vibrationally hot excited states. The transient bands become blue-shifted and narrow with time in the course of vibrational relaxation, which is complete in approx. 2 ps. Another, much weaker, bleach in the fingerprint region at $\sim 1500\text{ cm}^{-1}$ almost coincides with the appearance of a transient at $\sim 1480\text{ cm}^{-1}$.

The TRIR spectra of **4-C** and **4-SC** both show a bleach of the ester $\text{C}=\text{O}$ stretch at $\sim 1730\text{ cm}^{-1}$ with an associated lower energy transient at $\sim 1700\text{ cm}^{-1}$ for **4-C**, similar to that observed previously for a related $\text{Pt}(\text{bipyester})\text{bis}(\text{acetylide})$ ^[51,52], and $\sim 1710\text{ cm}^{-1}$ for **4-C**, consistently with the population of the antibonding orbital of the CO group upon excitation. The broadness of the $\nu(\text{CO})$ in the excited state of **4-C** is due to an overlap of a symmetric/asymmetric combination of the stretching vibrations of the two CO groups.

Of particular interest is that the intensity of the bleach and transient is significantly lower in **4-SC** if compared to **4-C**, the apparent shift in the frequency is significantly smaller, and no broadening of the $\nu(\text{CO})$ is observed (Figure 7). The presence of the methylene spacer prevents conjugation of the ester $\text{C}=\text{O}$ π -bond from the aromatic bipy rings, thus reducing electronic communication. However, the presence of the bleach and associated transient in the TRIR indicates that the ester group is still affected by the redistribution of electron density upon excitation, probably due to increase of electron density on the bipy itself, or due to somewhat delocalised structure of the excited state (the latter in accord with the broad and intense $\nu(\text{CC})$ bands in the excited state, insets in Figure 6).

It is also evident from Figure 6 that intensity of the IR signals in the excited state is considerably higher than in the ground state. Such increase in transition probability for virtually all transitions observed could be explained by, for example, structural and / or electronic delocalisation in the excited state. For example, the FTIR spectrum of **4-SP** and **4-SC** (Figure 6, bottom), differently to the spectra of **4-P** and **4-C**, shows two clearly resolved bands at ~ 1600 and 1620 cm^{-1} , which are due to breathing modes of the bipyridyl, and of the Ph ring of the acetylide ligand. DFT calculations demonstrate that in the ground state these two vibrations albeit very close in energy are decoupled. In the lowest triplet state, however, calculations show that these vibrations are strongly coupled, which causes the observed 10-times increase in the intensity of vibrations between ~ 1550 and 1590 cm^{-1} .

The above results are consistent with a bipy π^* based LUMO. The population of an antibonding π^* orbital would result in a decrease in bond order within the bipy skeleton, reducing the energy of vibrations associated with these bonds. The lower energy transients assigned to bipy ring vibrations, the intense nature of the transient peaks associated with the bipy ring, as well as the lower energy transient observed for the conjugated $\text{C}=\text{O}$ moiety in **4-C** support this hypothesis.

FULL PAPER

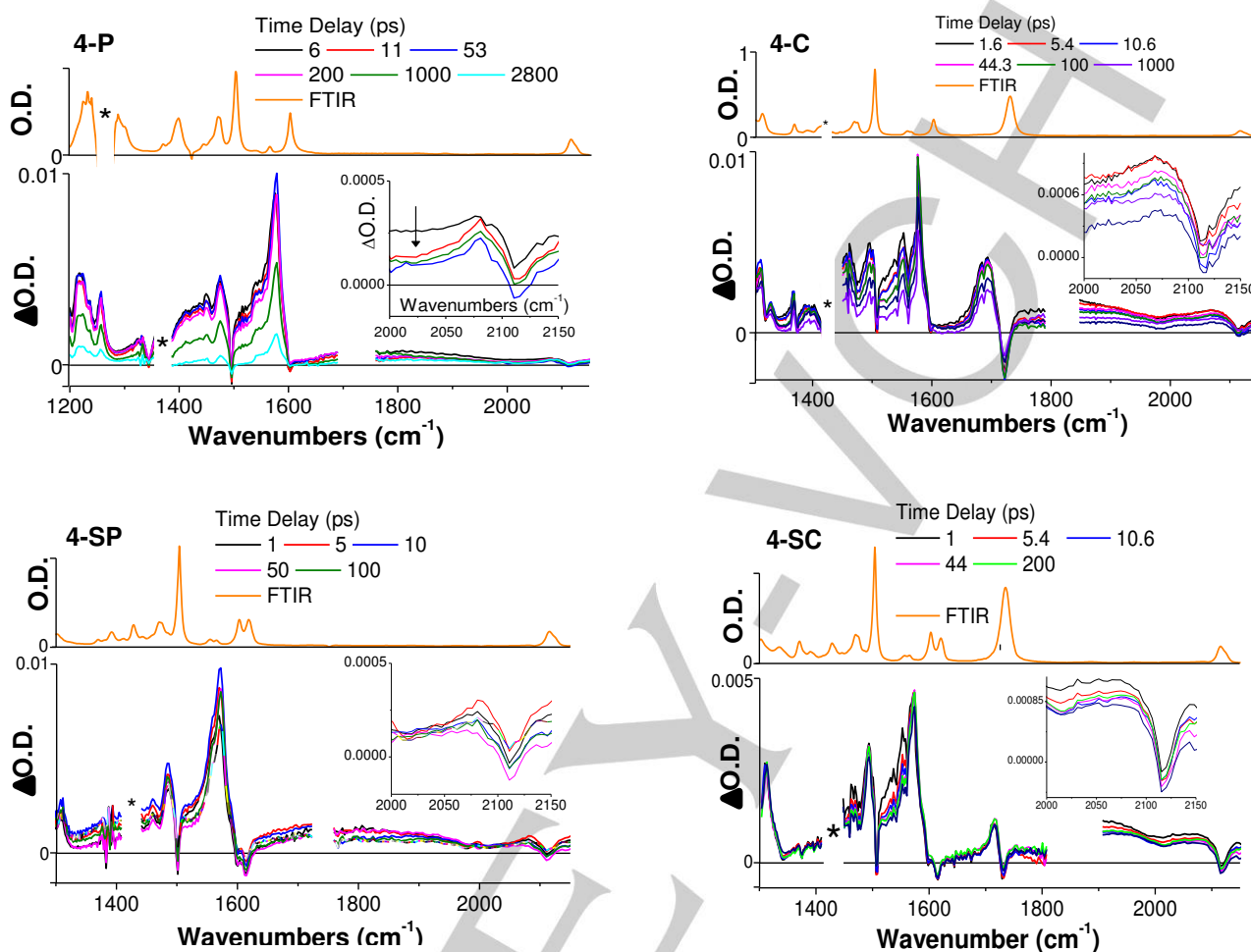


Figure 6 Picosecond TRIR data for all complexes in CD_2Cl_2 . The offset line shows the ground state FTIR spectrum recorded in CH_2Cl_2 , at 1/1000 intensity

In the 2000 cm^{-1} region, the TRIR data for all complexes are qualitatively similar, combining a bleach at $\sim 2120\text{ cm}^{-1}$ of both antisymmetric/symmetric combinations of the $\nu(\text{CC})$ with a broad absorption between $\sim 1800\text{--}2000\text{ cm}^{-1}$. This broad feature has been previously assigned to vibrations associated with the “oxidized” platinum acetylide subunit formed in the CT state^[23]. The shift of the acetylide vibration to lower energy upon excitation is consistent with the assignments of a Pt-acetylide localised HOMO, which is depopulated upon excitation. Due to the above-mentioned delocalisation in the excited state, the intensity of the asymmetric $\nu(\text{CC})$ combination is ~ 100 -fold higher than in the ground state (see SI for calculated IR spectra of the lowest triplet state in all complexes). In the experimental spectrum this transition appears as a very broad band across the entire $1600\text{--}2000\text{ cm}^{-1}$ range. The broadness of this band may be explained by a large number of conformations, and anharmonic coupling to intramolecular low-frequency modes, and to the low frequency solvent modes.

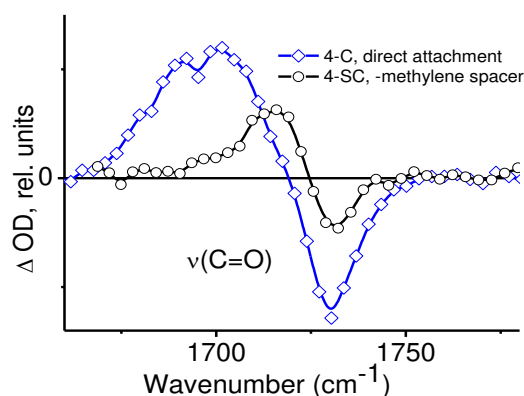


Figure 7. Comparison between spectral shape of the TRIR spectra in the region of $\nu(\text{CO})$ of the ester group between complexes with direct attachment of esters (blue \diamond , 4-C) vs. decoupled (black \circ , 4-SC). Data in DCM, following ~ 50 fs, 400 nm excitation, time delay between the pump and the probe 100 ps.

FULL PAPER

In transition-metal complexes ultrafast intersystem crossing following the population of a singlet Frank-Condon state usually leads to population of vibrationally hot triplet states^[53–57]. The lack of significant spectral evolution on the >500 fs time-scale of TRIR experiment indicates that intersystem crossing in the ML/LL'CT state of **4** also occurs on a sub-picosecond timescale^[58].

The dynamics of the excited states in all complexes studied (Figure 8) comprises an ultrafast vibrational relaxation of a few picoseconds discussed above, as well as a component of approx. 19 ps. The latter can be attributed to intramolecular structural reorganisation concomitant with vibrational relaxation of the hot triplet excited state. This structural change is reflected in a slight redistribution of intensity between vibrational bands with time. Since the shape of the TRIR spectra attained by ca. 100 ps in all complexes then persists on the ~ 2.5 ns time scale, the spectral shape evolution cannot be attributed to vibrational cooling. The excited state lifetimes of **4-P** and **4-C** are ~ 2 ns and 1.7 ns, resp. It is worth noting that the absorption and emission spectra, and the lifetimes of the excited state in **4-SP** and **4-SC** are very similar to one another, and to that of Pt(Bu₂-bipy)(-CC-Ph-OMe)^[47].

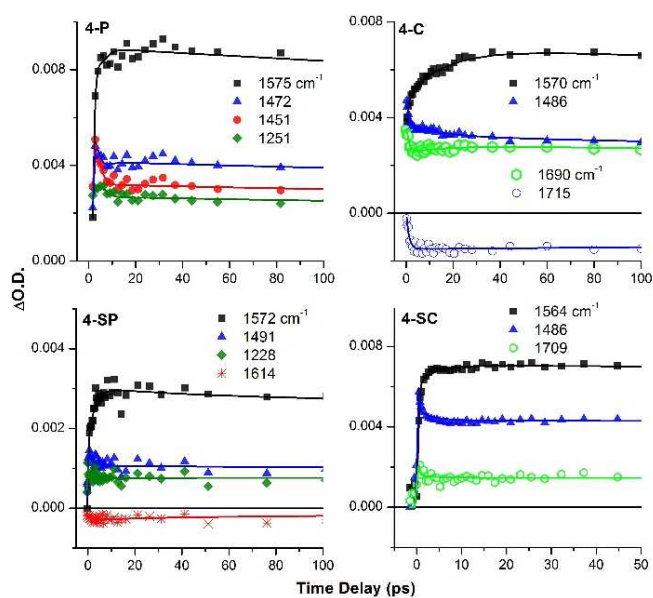


Figure 8 Kinetic traces obtained at selected frequencies from the TRIR data in Fig 6, for **4-P** and **4-SP** (left), and **4-C** and **4-SC** (right). Symbols – experimental data, solid lines – biexponential fit to the data with the parameters stated in Table 1. The band at 1614 cm⁻¹ (*) corresponds to a bipy-localised vibration in the ground state of **4-SP**. The bands at 1564–1575 (■) and 1450–1491 cm⁻¹ (▲) correspond to several of the delocalised bipyridil-acetylide-ring stretching vibrations of the excited state; 1228–1251 cm⁻¹ correspond to a coupled –P=O/bipy mode of the excited state (♦). 1690 and 1709 cm⁻¹ (-○-) correspond to the –C=O stretching vibrations in the excited state of **4-C** and **4-SC**, resp.

The synchronous dynamics of different vibrations across the molecules, which involve the entire [bipy-Pt-CC-Ph] framework is again consistent with the delocalised structure of the excited state, and that the spectral features observed correspond to one excited state throughout. Such delocalisation may be responsible for an increased intensity of the IR transitions in the excited state.

Ultrafast Electronic Transient Absorption Spectroscopy

The observations of the excited state dynamics have also been confirmed by transient absorption studies in the range 380 – 1400 nm, (Fig. 9 and Fig. S22-S24). Upon excitation with a ~40 fs, 400 nm laser pulse, the UV/vis region of the transient spectrum shows features typical for coordinated bipyridyl radical-anions at ~390, 520, and ~650 nm. The presence of the oxidised

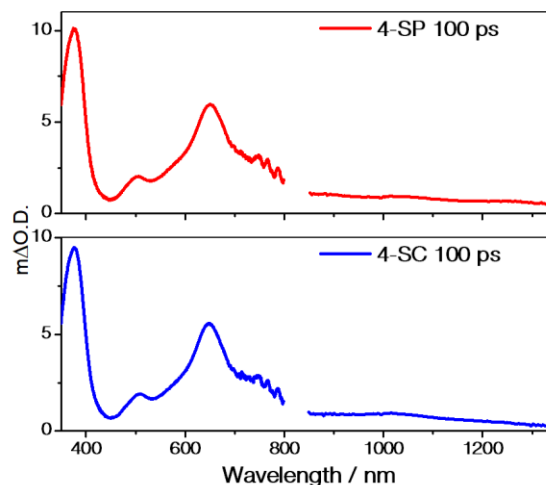


Figure 9 Selected transient absorption spectra of **4-SP** and **4-SC** across the visible and NIR regions recorded in dichloromethane.

[Pt(acetylide)] moiety is evident from a broad, structureless (**4-SP**, **4-SC**) band which continues into the NIR region and does not decay whatsoever by 1400 nm – an observation consistent with previous work on similar systems^[59]. This low energy absorption band is responsible for the “offset” observed in the TRIR spectra discussed above. The extremely broad low-energy absorption band is consistent with the highly delocalised nature of the excited state in all cases. The lifetimes of the excited states obtained from the TA data are the same, within experimental error, as those obtained from TRIR and/or emission spectroscopy, confirming that the same lowest excited state is observed in all cases.

Conclusions

The effect of electronically decoupling protected anchoring groups from the light-absorbing metal complex core has been explored for Pt(II) complexes. Pt(4-R₂-bipy)(acetylide)₂, containing electron-withdrawing groups R = phosphonate or carboxylate, attached in two different ways, either directly or via a saturated CH₂- spacer which permits free rotation of the R-group, have been synthesized and characterized by emission and absorption spectroscopy, and electrochemistry. The nature and dynamics of the excited state has been investigated by femtosecond Time-Resolved Infrared and Transient Absorption spectroscopy. Vibrational signatures and dynamics of charge-transfer states have been identified; the assignment of electronic states and their vibrational origin was aided by TDDFT calculations.

FULL PAPER

Ultrafast energy re-distribution accompanied by structural changes was detected by TRIR. There are unexpected, significant differences between the structures of the charge-transfer excited states, as well as the differences in the structural reorganisation in the complexes bearing directly attached vs. decoupled anchoring groups.

The observed shift of $\nu(\text{CO})$ and $\nu(\text{PO})$ vibrations to low frequencies upon excitation due to population of the antibonding orbitals, and the shift to lower energies of symmetric/ asymmetric combination of $\nu(\text{CC})$ of the acetylide ligands, confirm the Charge-Transfer-to-diimine, ML/LL'CT, nature of the lowest excited state. The extremely intense and broad $\nu(\text{CC})_{\text{s/a}}$ in the charge-transfer excited states, with the incredibly large shifts of $\sim(-60)$ cm^{-1} , and $\sim(-300)$ cm^{-1} , resp. compared to the ground state $\nu(\text{CC})_{\text{s/a}}$, which persist on the nanosecond timescale, indicates a presence of a delocalised $\{-\text{CC}-\text{Pt}-\text{CC}-\}$ moiety in ML/LL'CT.

The introduction of the $-\text{CH}_2$ spacer between the bipy ring and the electron-withdrawing anchoring group R has drastic effects on the photophysical properties of the compounds: it makes them much more akin to the compounds bearing electron-donating alkyl substituents on the diimine ligand. The lifetime of the $^3\text{ML/LL'CT}$ excited state increases 10-fold, from ~ 2 ns to ~ 20 ns, between **4-C/4-P** and **4-SC/4-SP**, due to electron donating nature of the methylene spacer resulting in a higher energy LUMO, increasing the energy of the excited state (confirmed by the change in $E^{1/2}_{\text{red}}$, and a shift of emission maxima to 640 nm vs. 710 nm), and reducing the rate of non-radiative decay in line with the energy gap law.

The shift of the $\nu(\text{CO})$ energy upon excitation group is considerably larger, by ~ 20 cm^{-1} , in $-\text{C}(\text{O})\text{OEt}$ vs. $-\text{CH}_2-\text{C}(\text{O})\text{OEt}$, again indicating the influence of the $-\text{CH}_2$ spacer. Importantly, the small but explicit downward shift of $\nu(\text{CO})$ in $-\text{CH}_2-\text{C}(\text{O})\text{OEt}$, in TRIR spectra confirm that the ester group in **4-SC** is still affected by the electron density redistribution in the excited state despite introduction of such saturated $-\text{CH}_2-$ spacer. A combination of DFT and TD-DFT calculations provide a qualitative rationale for the nature of the electronic and vibrational spectra observed, and suggest a somewhat delocalised nature of the lowest CT excited state even in the case of the compounds bearing $-\text{CH}_2-$ spacer. Such delocalisation accounts for >10 -fold enhancement of the majority of IR-transitions in the excited state compared to the ground state, and for the vast broadness of the $\nu(\text{CC})$ in the CT state.

This work demonstrates that decoupling of the anchoring group from the diimine via a saturated spacer is an easy approach that permits combining a higher reduction potential and 10-fold longer charge-transfer excited state lifetime with the possibility of surface attachment, whilst retaining electron transfer photoreactivity.

Experimental Section

UV/VIS Absorption spectra were recorded using a Cary 50 Bio spectrometer running the Cary WinUV Scan application. A 1 cm path length quartz cell was used for all measurements.

Cyclic Voltammetry

Experiments were carried out using an Autolab Potentiostat 100 controlled by a PC running the GPES v.4.9 application. All measurements were performed using an Ag/AgCl reference electrode and a platinum wire counter electrode. A glassy carbon working electrode was used for 4-P, 4-SP, and 4-C, and a platinum disc working electrode for 4-SP. The $[\text{TBA}][\text{PF}_6]$ electrolyte was obtained from commercial sources and recrystallised prior to use.

Emission spectroscopy

Emission spectra were recorded on a Horiba Jobin&Yvon Fluoromax-4 spectrometer. Emission lifetimes were recorded on an Edinburgh Instruments Mini- τ with a ~ 75 ps pulse diode laser (410 nm) as an excitation source. Samples were degassed using three freeze-pump-thaw cycles. Emission quantum yields were calculated with respect to the standard $[\text{Ru}(\text{bipy})_3]\text{Cl}_2 \cdot 6\text{H}_2\text{O}$ in water. See the SI for full details.

Fourier Transform Infrared Spectroscopy and Time-Resolved Infrared Spectroscopy

FTIR spectroscopy was carried out using a Perkin-Elmer FTIR spectrophotometer controlled by a PC running Perkin-Elmer software Spectrum, version 3.02. Picosecond TRIR studies were performed in the Ultrafast Spectroscopy Laboratory, Rutherford Appleton Laboratory, STFC, UK, ULTRA^[60] facility. The IR spectrometer comprised two synchronized 10kHz, 8 W, 40 fs and 2 ps Ti:Sapphire oscillator/regenerative amplifiers (Thales) which pump a range of optical parametric amplifiers (TOPAS). A portion of the 40 fs Ti:Sapphire beam was used to generate tuneable mid-IR probe light with around 400 cm^{-1} bandwidth. The 400 nm pump beam was generated from the second harmonic of the 40 fs laser. The instrumental response function for TRIR measurements is approximately 250 fs. The probe and pump beam diameters in the sample were about 70 and 150 μm , respectively, and the pump energy at the sample was 1 to 1.5 μJ . In this case changes in IR absorption spectra were recorded by three HgCdTe linear-IR array detectors on a shot-by-shot basis. All experiments were carried out in Harrick cells with 2 mm thick CaF_2 windows with 500 to 950 μm sample path length and a typical optical density of 0.5 to 1 at 400 nm. All samples were mounted on a 2D-raster stage and solutions were flowed through the cell to ensure photostability. Data processing and global analysis were carried out using Origin 7.0 and Glotaran 1.5.1.

Ultrafast Transient Absorption

Ultrafast Transient Absorption setup comprises of a commercial detection instrument (Helios, Ultrafast Systems) as well as the following light sources: 84 MHz Ti:Sapphire 25 fs 800 nm seed laser (Mai Tai Spectra Physics), Ti:Sapphire chirped-pulse amplifier repetition rate 10 KHz, 12W average power and nominal pulse duration 40 fs (Spitfire Ace PA-40) both from Spectra-Physics; frequency doubling and tripling achieved by a commercial instrument utilising beta-Barium-Borate crystals (TimePlate, by Photop Technologies); UV-Vis-NIR generation has been done by means of Optical Parametric Amplification (Topas Prime, by Light Conversion). The latter two served as quasi monochromatic excitation pump sources, selectable from 235 nm to 1600 nm. Probe beam is a white light supercontinuum generated *in-situ* and optimised for UV (340-750 nm), Vis (450-950 nm) and NIR (800-1600 nm) regions. Detection was performed by virtue of CMOS and InGaAs sensors for UV/Vis and NIR grating-dispersed spectra, respectively. Dynamics were fitted using global analysis in Glotaran 1.5.1.

FULL PAPER

Computational Methods

All calculations were performed using the Gaussian 09 software package, version C.01^[61]. Gaussian was compiled using the Portland compiler v 8.0-2 on an EMT64 architecture using Gaussian-supplied versions of BLAS and ATLAS^[62,63]. All calculations utilized the B3LYP functional^[64]. The 6-311G** basis set^[65,66] was employed for all elements except Platinum, for which a Stuttgart-Dresden pseudo-potential was instead used^[67]. This combination of basis sets has been found to provide a reasonably accurate description of the properties and behaviour of transition-metal complexes in our previous work^[68,69]. In all calculations, the solvent was described using the polarizable continuum model (PCM), as implemented in Gaussian^[70,71]. For all calculations, an "ultrafine" integral grid was used and no symmetry constraints were applied. All optimized geometries were confirmed as local minima by the absence of imaginary frequencies in their calculated vibrational spectra, within the harmonic approximation. Vibrational frequencies were scaled by 0.981 for the majority of the spectrum and 0.967 in the acetylide region, to account for anharmonicity^[69,72,73]. Vibrational spectra were generated using software developed in-house. A description of the procedures used in the calculations is given in the SI.

Synthesis

Unless otherwise stated, all starting materials were obtained from commercial sources and used without further purification, and standard Schlenk techniques were used for all syntheses.

Ligands and Complexes

4,4'-bis(carboxyl)-2,2'-bipyridine: 4,4'-dimethyl-2,2'-bipyridine (2.5 g, 13.5 mmol) was dissolved in 100 mL of 98% H₂SO₄ in air. To this solution, potassium dichromate (12 g) was added in portions whilst stirring, ensuring the temperature remained between 40-80°C. Once the dichromate addition was complete, the mixture was cooled in an ice bath, and the resulting precipitate filtered off using a glass sinter funnel. The precipitate was then refluxed for 16 h in 50% HNO₃ (50 mL), then poured over ~200 g of ice and diluted to ~400 mL with water. Once the ice melted, the resulting white precipitate was filtered off, washed with water and acetone and dried under a vacuum. Yield 2.29 g (91%). ¹H NMR (400 MHz, DMSO) δ 8.93 (dd, *J* = 4.9, 0.7 Hz, 2H), 8.87 – 8.83 (m, 2H), 7.92 (dd, *J* = 4.9, 1.6 Hz, 2H).

Compounds **1a-d** were prepared according to a modified literature procedure^[11].

4,4'-bis(ethylcarboxy)-2,2'-bipyridine (1a): 4,4'-bis(carboxyl)-2,2'-bipyridine (1.05 g, 4.12 mmol) was suspended in 40 mL ethanol and 2 mL of 98% H₂SO₄ added. The mixture was refluxed at 85°C under argon for 24 h to give a pale pink solution. Removal of the solvent under vacuum left a pale pink oil, which was mixed with water (20 mL) and extracted with chloroform (3 x 50 mL). The combined organic fractions were dried with MgSO₄, filtered and the solvent volume reduced under vacuum to approximately 20 mL. Addition of methanol (20 mL) resulted in formation of a pale pink precipitate, which was filtered off on a sinter and dried under vacuum. Yield 964 mg (76%). ¹H NMR (400 MHz, CDCl₃) δ 8.97 (s, 2H), 8.89 (d, *J* = 4.9 Hz, 2H), 7.94 (dd, *J* = 5.0, 1.6 Hz, 2H), 4.48 (q, *J* = 7.1 Hz, 4H), 1.47 (t, *J* = 9.2, 5.0 Hz, 6H).

4,4'-bis(hydroxymethyl)-2,2'-bipyridine (1b): **1a** (750 mg, 2.4 mmol) was suspended in ethanol (50 mL) followed by the addition of sodium borohydride (2g, 53 mmol). The mixture was refluxed at 65°C under argon for 3 h. A gel was observed forming on the surface of the reaction mixture

after approximately 1 hour. An additional 25 mL of ethanol were added to dissolve the gel. After cooling to room temperature, saturated NH₄Cl_(aq) (100 mL) was added to the mixture and stirred for 15 min. The ethanol was removed under vacuum and the resulting white precipitate was dissolved in the minimum quantity of water (approx. 150 mL). The solution was extracted with ethyl acetate (5 x 50 mL) and the combined organic fractions dried of MgSO₄. The solvent was removed under vacuum resulting in a pale pink solid. Yield 306 mg (50%). ¹H NMR (400 MHz, DMSO) δ 8.60 (d, *J* = 4.9 Hz, 2H), 8.39 (s, 2H), 7.40 – 7.34 (m, 2H), 5.56 (t, *J* = 5.8 Hz, 2H), 4.63 (d, *J* = 5.8 Hz, 4H).

4,4'-bis(bromomethyl)-2,2'-bipyridine (1c): **1b** (674 mg, 3.12 mmol) was dissolved in 48% HBr (40 mL) and 98% H₂SO₄ (14 mL). The resulting orange fuming solution was refluxed at 100°C for 18 h. Upon cooling to room temperature, the mixture was neutralized with saturated NaOH_(aq) (approx. 200 mL). The resulting white precipitate was filtered off using a sinter and washed with water (300 mL) and air dried. The solid was then dissolved in chloroform (40 mL), dried over MgSO₄ and filtered. The solvent was removed under vacuum leaving a white solid. Yield 842 mg (79%). ¹H NMR (400 MHz, CDCl₃) δ 8.70 (d, *J* = 5.0 Hz, 2H), 8.46 (d, *J* = 1.2 Hz, 2H), 7.39 (dd, *J* = 5.0, 1.8 Hz, 2H), 4.51 (s, 4H).

4,4'-bis(diethoxymethylphosphonato)-2,2'-bipyridine (1e): Chloroform (10 mL) was mixed with diethyl phosphite (15 mL) and sparged with dry nitrogen for 30 min. This mixture was transferred to a flask containing **1c** (842 mg, 2.46 mmol) and refluxed at 85°C for 6 hours. After cooling to room temperature the chloroform and diethyl phosphite were removed under vacuum leaving a pale pink solid. The crude product was purified using silica gel column chromatography (80:20 v/v Ethyl Acetate:MeOH eluent) to give a pale yellow oil, which crystallized overnight to an off-white solid. Yield 942 mg (64%). ¹H NMR (250 MHz, CDCl₃) δ 8.60 (d, *J* = 5.0 Hz, 2H), 8.33 (s, 2H), 7.42 – 7.28 (m, 2H), 4.07 (dq, *J* = 8.1, 7.1 Hz, 8H), 3.23 (d, *J* = 22.2 Hz, 4H), 1.27 (t, *J* = 7.1 Hz, 12H). ³¹P NMR (101 MHz, CDCl₃) δ 24.30 (s). MS (ESI, +ve): *m/z* 457.2 (MH⁺).

4,4'-bis(diethoxyphosphonato)-2,2'-bipyridine (2a): **2a** was prepared according to a modified literature procedure^[9]. Anhydrous toluene (15 mL), triethylamine (3 mL) and diethyl phosphite (0.35 mL, 2.7 mmol) were mixed and sparged with argon for 30 min. This mixture was transferred via syringe to a flask containing 4,4'-dibromo-2,2'-bipyridine (296 mg, 0.94 mmol), triphenylphosphine (2.6 g, 10 mmol) and Pd(PPh₃)₄ (130 mg, 0.11 mmol) under an Ar atmosphere, then refluxed at 100°C for 7 h. Upon cooling to room temperature, toluene (10 mL) was added to dissolve a gel-like precipitate which had formed, then the resulting solution washed with saturated NH₄Cl (2 x 20 mL) and water (2 x 50 mL). The organic fraction was dried over MgSO₄ and the solvent removed under vacuum to leave an off-white powder. The crude product was purified by gradient elution silica gel column chromatography. Dichloromethane was used as the initial eluent to remove the triphenylphosphine which elutes with the solvent front, followed by 3% v/v methanol in dichloromethane to yield an off-white powder. Yield 266 mg (66%). ¹H NMR (400 MHz, CDCl₃) δ 8.87 (t, *J* = 5.1 Hz, 2H), 8.80 (d, *J* = 14.2 Hz, 2H), 7.76 (ddd, *J* = 13.0, 4.8, 1.3 Hz, 2H), 4.32 – 4.12 (m, 8H), 1.39 (t, *J* = 7.1 Hz, 12H). ³¹P NMR (101 MHz, CDCl₃) δ 14.57 (s). MS (ESI, +ve): *m/z* 429.8 (MH⁺).

4,4'-bis(methylcarboxy)-2,2'-bipyridine (3a): Prepared according to a modified literature procedure^[9]. All glassware was flame dried before use. Diisopropylamine (1.05 mL, 8 mmol) was dissolved in dry THF (15 mL) and cooled to -78°C. 1.6M n-butyllithium in hexane (4.1 mL, 6.5 mmol) was added dropwise to this in two portions and stirred for 20 min, resulting in a deep red solution. This was transferred via a cannula over 30 min to a solution of 4,4'-dimethyl-2,2'-bipyridine (500 mg, 2.7 mmol) in dry THF (15 mL) which had also been cooled to -78°C. This mixture was stirred at -78°C for 2 h. CO_{2(g)} was bubbled through the solution for 15 min resulting

FULL PAPER

in the immediate formation of a pale yellow precipitate. Upon warming to room temperature, the THF was removed under vacuum leaving a pale yellow solid. This was dissolved in water (10 mL) and washed with dichloromethane (3 x 50 mL). The aqueous layer was carefully acidified with 2M HCl (to pH 2-3) and the water removed under vacuum leaving a wet yellow solid. Attempts to remove the remaining water under high vacuum were unsuccessful, resulting in a yield over 300%. This product was used in the next step without any further attempt at purification. ¹H NMR (400 MHz, D₂O) δ 8.64 (d, *J* = 5.5 Hz, 2H), 8.24 (s, 2H), 7.74 – 7.68 (m, 2H), 3.96 – 3.93 (m, 4H).

4,4'-bis(ethoxymethylcarbonyl)-2,2'-bipyridine (3b): 3a (1.63g, crude) was dissolved in ethanol (80 mL) and 98% H₂SO₄ (4 mL). This was refluxed at 80°C for 72 h. Upon cooling to room temperature, the ethanol was removed under vacuum and water (100 mL) was added to the flask resulting in a white precipitate. This was extracted with dichloromethane (5 x 30 mL) and the combined organic fractions dried over MgSO₄. The solvent was removed under vacuum resulting in a pale pink solid. Yield 512 mg (26% w.r.t. 4,4'-dimethyl-2,2'-bipyridine from **3a**). ¹H NMR (400 MHz, CDCl₃) δ 8.65 (d, *J* = 5.0 Hz, 2H), 8.35 (d, *J* = 0.8 Hz, 2H), 7.31 (dd, *J* = 5.0, 1.7 Hz, 2H), 4.20 (q, *J* = 7.1 Hz, 4H), 3.74 (s, 4H), 1.28 (t, *J* = 7.1 Hz, 6H). MS (ESI, +ve) *m/z* = 328.

Pt(4,4'-bis(diethoxymethylphosphonato)-2,2'-bipyridine)Cl₂ (4a): 1d (50 mg, 0.11 mmol) and Pt(DMSO)₂Cl₂ (46 mg, 0.11 mmol) were placed under argon and then dissolved in ethanol (10 mL) previously sparged with argon for 30 min. The solution was then refluxed at 65°C under argon for 24 h resulting in a yellow solution. Upon cooling to room temperature, hexane (40 mL) was added, giving a yellow precipitate which was filtered off on a sinter, washed with 3 x 25 mL ice cold ethanol and dried under vacuum. Yield 57 mg (72%) ¹H NMR (250 MHz, CDCl₃) δ 9.05 (d, *J* = 6.1 Hz, 2H), 8.04 (s, 2H), 7.36 (dt, *J* = 5.9, 1.9 Hz, 2H), 4.14 (dq, *J* = 8.4, 7.1 Hz, 8H), 3.34 (d, *J* = 22.4 Hz, 4H), 1.33 (t, *J* = 7.1 Hz, 12H). ³¹P NMR (101 MHz, CDCl₃) δ 21.55 (s). MS (TOF +ve): *m/z* 723.1 (MH⁺) Calculated elemental analysis: C 33.25; H 4.19; N 3.88, Found: C 31.68; H 4.16; N 3.50.

Pt(4,4'-bis(diethoxymethylphosphonato)-2,2'-bipyridine)bis(4-ethynylpentylloxybenzene) (4-SP): 4a (86 mg, 0.18 mmol) and copper (I) iodide (3.4 mg, 0.02 mmol) were placed under argon and dissolved in dry dichloromethane (30 mL) previously sparged with argon for 15 min. 4-ethynylpentylloxybenzene (117 μL, 0.6 mmol) and diisopropylamine (2 mL) were added via syringes. The solution immediately changed colour from yellow to orange and was stirred at room temperature for 72 h. The solvent was then removed under vacuum leaving an orange residue. This was redissolved in dichloromethane (20 mL) and the solution washed with 1:25 acetic acid:water (25 mL), water (25 mL), 0.2M sodium hydroxide (25 mL) and finally water (2 x 50 mL). The organic fraction was dried over MgSO₄, filtered and the solvent removed under vacuum, resulting in a bright red solid. The crude product was purified using silica gel chromatography (eluent 5% v/v methanol in dichloromethane). Yield 117 mg (63%). ¹H NMR (400 MHz, CDCl₃) δ 9.27 (d, *J* = 5.7 Hz, 2H), 8.09 (s, 2H), 7.42 (d, *J* = 8.7 Hz, 4H), 7.32 (d, *J* = 5.7 Hz, 2H), 6.81 (d, *J* = 8.8 Hz, 4H), 4.06 – 3.90 (m, 12H), 3.23 (d, *J* = 22.1 Hz, 4H), 1.83 – 1.73 (m, 4H), 1.51 – 1.35 (m, 8H), 1.22 (t, *J* = 7.1 Hz, 12H), 0.93 (t, *J* = 7.1 Hz, 6H). ³¹P NMR (101 MHz, CDCl₃) δ 11.92 (s). MS (TOF +ve): *m/z* 1026.1 (MH⁺). Calculated elemental analysis C 53.85; H 5.89; N 2.73, Found C 53.66; H 5.84; N 2.71.

Pt(4,4'-bis(diethoxyphosphonato)-2,2'-bipyridine)Cl₂ (5a): 2 (108 mg, 0.25 mmol) and Pt(DMSO)₂Cl₂ (100 mg, 0.25 mmol) were placed under argon and then dissolved in ethanol (20 mL) previously sparged with argon for 30 min. The solution was then refluxed at 65°C under argon for 24 h resulting in an orange solution. Upon cooling to room temperature an orange precipitate appeared. Hexane (50 mL) was added and the

precipitate filtered off on a sinter, washed with 3 x 25 mL ice cold ethanol and dried under vacuum. Yield 154 mg (88%). ¹H NMR (250 MHz, CDCl₃) δ 9.55 (dd, *J* = 5.7, 4.1 Hz, 1H), 8.38 (d, *J* = 13.4 Hz, 1H), 7.82 (ddd, *J* = 12.3, 5.9, 1.4 Hz, 1H), 4.45 – 4.12 (m, 1H), 1.42 (t, *J* = 7.1 Hz, 1H). ³¹P NMR (101 MHz, CDCl₃) δ 11.27 (s). MS (MALDI) *m/z* = 693.

Pt(4,4'-bis(diethoxyphosphonato)-2,2'-bipyridine)bis(4-ethynylpentylloxybenzene) – (4-P): 5a (154 mg, 0.22 mmol) and copper (I) iodide (3.5 mg, 0.02 mmol) were dissolved in dry dichloromethane (20 mL) previously sparged with argon for 15 min. 4-ethynylpentylloxybenzene (130 μL, 0.66 mmol) and diisopropylamine (2 mL) were added via syringes. The solution immediately changed colour from orange to red and was stirred at room temperature for 72 h. The solvent was then removed under vacuum leaving a deep red residue. This was redissolved in dichloromethane (20 mL) and the solution washed with 1:25 acetic acid:water (25 mL), water (25 mL), 0.2M sodium hydroxide (25 mL) and finally water (2 x 50 mL). The organic fraction was dried over MgSO₄, filtered and the solvent removed under vacuum, resulting in a bright red solid. The crude product was purified using silica gel chromatography (eluent 5% v/v methanol in dichloromethane). Yield 221 mg (98%). ¹H NMR (250 MHz, CDCl₃) δ 10.19 – 9.96 (m, 2H), 8.51 (d, *J* = 13.5 Hz, 2H), 7.91 (ddd, *J* = 12.5, 5.6, 1.2 Hz, 2H), 7.53 – 7.37 (m, 4H), 6.89 – 6.75 (m, 4H), 4.43 – 4.12 (m, 8H), 3.97 (t, *J* = 6.6 Hz, 4H), 1.92 – 1.69 (m, 4H), 1.54 – 1.29 (m, 20H), 0.95 (t, *J* = 7.0 Hz, 6H). ³¹P NMR (101 MHz, CDCl₃) δ 11.92 (s). MS (TOF +ve): *m/z* 998.2 (MH⁺) Calculated elemental analysis: C 52.96; H 5.66; N 2.76, Found: C 52.38; H 5.80; N 2.76.

Pt(4,4'-bis(ethoxymethylcarbonyl)-2,2'-bipyridine)Cl₂ (6a): 3b (250 mg, 0.76 mmol) and Pt(DMSO)₂Cl₂ (321 mg, 0.76 mmol) were placed under argon and then dissolved in ethanol (10 mL) previously sparged with argon for 30 min. The solution was then refluxed at 65°C under argon for 24 h resulting in yellow solution. Upon cooling to room temperature hexane (50 mL) was added and the precipitate filtered off on a sinter, washed with 3 x 25 mL ice cold ethanol and dried under vacuum. Yield 411 mg (91%). ¹H NMR (400 MHz, CDCl₃) δ 9.24 (d, *J* = 6.0 Hz, 2H), 8.10 (d, *J* = 1.6 Hz, 2H), 7.41 (dd, *J* = 6.1, 1.7 Hz, 2H), 4.28 (q, *J* = 7.1 Hz, 4H), 3.86 (s, 3H), 1.35 (t, *J* = 7.1 Hz, 6H). MS (EI): *m/z* 593.9 (M⁺) Calculated elemental analysis: C 36.37; H 3.39; N 4.71, Found: C 35.56; H 3.14; N 4.55.

Pt(4,4'-bis(ethoxymethylcarbonyl)-2,2'-bipyridine)bis(4-ethynylpentylloxybenzene) (4-SC): 6a (154 mg, 0.22 mmol) and copper (I) iodide (3.5 mg, 0.02 mmol) were dissolved in dry dichloromethane (20 mL) and sparged with argon for 15 min. 4-ethynylpentylloxybenzene (130 μL, 0.66 mmol) and diisopropylamine (2 mL) were added via syringes. The solution immediately changed colour from yellow to orange and was stirred at room temperature for 72 h. The solvent was then removed under vacuum leaving an orange residue. This was redissolved in dichloromethane (20 mL) and the solution washed with 1:25 acetic acid:water (25 mL), water (25 mL), 0.2M sodium hydroxide (25 mL) and finally water (2 x 50 mL). The organic fraction was dried over MgSO₄, filtered and the solvent removed under vacuum, resulting in a dull orange solid. The crude product was purified using silica gel chromatography (eluent 3% v/v methanol in dichloromethane). Yield 101 mg (22%) ¹H NMR (400 MHz, CDCl₃) δ 9.56 (d, *J* = 5.6 Hz, 2H), 8.10 (s, 2H), 7.45 (d, *J* = 8.8 Hz, 4H), 7.40 (dd, *J* = 5.8, 1.5 Hz, 2H), 6.82 (d, *J* = 8.8 Hz, 4H), 4.21 (q, *J* = 7.1 Hz, 4H), 3.97 (t, *J* = 6.6 Hz, 4H), 3.80 (s, 4H), 1.86 – 1.74 (m, 4H), 1.52 – 1.35 (m, 8H), 1.30 (t, *J* = 7.1 Hz, 6H), 0.96 (t, *J* = 7.1 Hz, 6H). MS (EI): *m/z* 897.1 (M⁺). Calculated elemental analysis: C 36.37; H 3.39; N 4.71, Found: C 35.56; H 3.14; N 4.55.

Pt(4,4'-bis(ethylcarboxy)-2,2'-bipyridine)Cl₂ (7a): 1a (208 mg, 0.69 mmol) and Pt(DMSO)₂Cl₂ (293 mg, 0.69 mmol) were placed under argon and then dissolved in ethanol (20 mL) previously sparged with argon for 30 min. The solution was then refluxed for at 65°C under argon for 24 h

FULL PAPER

resulting in an orange solution. Upon cooling to room temperature, hexane (50 mL) was added and the resulting orange precipitate filtered off on a sinter, washed with 3 x 25 mL ice-cold ethanol and dried under vacuum. Yield 306 mg (78%). ¹H NMR (400 MHz, CDCl₃) δ 9.48 (d, *J* = 6.0 Hz, 2H), 8.45 (d, *J* = 1.5 Hz, 2H), 7.78 (dd, *J* = 6.0, 1.7 Hz, 2H), 4.13 (q, *J* = 7.1 Hz, 4H), 1.09 (t, *J* = 7.1 Hz, 6H). MS (TOF +ve): *m/z* 998.2 (MH⁺).

Pt(4,4'-bis(ethylcarboxy)-2,2'-bipyridine) bis(4-ethynylpentyloxybenzene) (4-C): 7a (153 mg, 0.22 mmol) and copper (I) iodide (5.7 mg, 0.03 mmol) were dissolved in dry dichloromethane (20 mL) previously sparged with argon for 15 min. 4-ethynylpentyloxybenzene (105 μL, 0.54 mmol) and diisopropylamine (2 mL) were added via syringes. The solution immediately changed colour from orange to red and was stirred at room temperature for 72 h. The solvent was then removed under vacuum leaving a deep red residue. This was redissolved in dichloromethane (20 mL) and the solution washed with 1:25 acetic acid:water (25 mL), water (25 mL), 0.2M sodium hydroxide (2 mL) and finally water (2 x 50 mL). The organic fraction was dried over MgSO₄, filtered and the solvent removed under vacuum, resulting in a bright red solid. The crude product was purified using silica gel chromatography (eluent 5% v/v methanol in dichloromethane). Yield 185 mg (78%). ¹H NMR (400 MHz, CDCl₃) δ 10.02 (d, *J* = 5.7 Hz, 2H), 8.63 (s, 2H), 8.09 (dd, *J* = 5.7, 1.5 Hz, 2H), 7.44 – 7.37 (m, 4H), 6.83 – 6.78 (m, 4H), 4.48 (q, *J* = 7.1 Hz, 4H), 3.96 (t, *J* = 6.6 Hz, 4H), 1.84 – 1.73 (m, 4H), 1.50 – 1.34 (m, 14H), 0.94 (t, *J* = 7.1 Hz, 6H). MS (FAB⁺ matrix) *m/z*: 670. Calculated elemental analysis: C 57.99; H 5.33; N 3.22, Found: C 59.11; H 5.69; N 2.83.

Acknowledgements

We thank the University of Sheffield, E-Futures Doctoral Training Centre, the EPSRC and the EPSRC Capital Equipment award, STFC, and Research Councils UK for funding. We thank Johnson-Matthey Plc for the generous supply of platinum salts. All calculations were performed on the "Sol" cluster of the Theoretical Chemistry Group at the University of Sheffield and on its central "Iceberg" cluster.

Keywords: platinum coordination compounds • photoinduced charge transfer • electron transfer • time-resolved infrared spectroscopy • computational chemistry

- [1] M. Hissler, J. E. McGarrah, W. B. Connick, D. K. Geiger, S. D. Cummings, R. Eisenberg, *Coord. Chem. Rev.* **2000**, *208*, 115–137.
- [2] S. Archer, J. A. Weinstein, *Coord. Chem. Rev.* **2012**, *256*, 2530–2561.
- [3] E. S. Andreiadis, M. Chavarot-Kerlidou, M. Fontecave, V. Artero, *Photochem. Photobiol.* **2011**, *87*, 946–964.
- [4] M. L. Muro, A. A. Rachford, X. Wang, F. N. Castellano, *Top. Organomet. Chem.* **2010**, *29*, 159–191.
- [5] A. Kudo, Y. Miseki, *Chem. Soc. Rev.* **2009**, *38*, 253–78.
- [6] I. Gillaizeau-gauthier, F. Odobel, M. Alebbi, R. Argazzi, E. Costa, C. A. Bignozzi, P. Qu, G. J. Meyer, T. De Nantes, N. Cedex, et al., *Inorg. Chem.* **2001**, *40*, 6073–9.
- [7] H. Park, E. Bae, J. Lee, J. Park, W. Choi, *J. Phys. Chem. B* **2006**, *110*, 8740–9.
- [8] E. Bae, W. Choi, J. Park, H. Shin, *J. Phys. ...* **2004**, 14093–14101.
- [9] S. Lense, K. I. Hardcastle, C. E. MacBeth, *Dalton Trans.* **2009**, 7396–401.
- [10] F. Lakadamyali, E. Reisner, *Chem. Commun.* **2011**, *47*, 1695–7.
- [11] V. Penicaud, F. Odobel, B. Bujoli, *Tetrahedron Lett.* **1998**, *39*, 3689–3692.
- [12] C. She, J. Guo, S. Irle, K. Morokuma, D. L. Mohler, H. Zabri, F. Odobel, K. Youm, F. Liu, J. T. Hupp, et al., *J. Phys. Chem. A* **2007**, *111*, 6832–42.
- [13] A. Islam, H. Sugihara, K. Hara, L. P. Singh, R. Katoh, Y. Takahashi, S. Murata, H. Arakawa, *New J. Chem.* **2000**, *24*, 343–345.
- [14] A. Islam, H. Sugihara, K. Hara, L. P. Singh, R. Katoh, M. Yanagida, Y. Takahashi, S. Murata, H. Arakawa, S. Osaka, et al., *Inorg. Chem.* **2001**, *40*, 5371–80.
- [15] E. A. M. Geary, N. Hirata, J. Clifford, J. R. Durrant, S. Parsons, A. Dawson, L. J. Yellowlees, N. Robertson, J. Yellowlees, *Dalt. Trans.* **2003**, 3757–3762.
- [16] E. A. M. Geary, L. J. Yellowlees, L. A. Jack, I. D. H. Oswald, S. Parsons, N. Hirata, J. R. Durrant, N. Robertson, *Inorg. Chem.* **2005**, *44*, 242–250.
- [17] F. Guo, Y. Kim, J. R. Reynolds, K. S. Schanze, *Chem. Commun.* **2006**, 1887–9.
- [18] E. A. M. Geary, K. L. McCall, A. Turner, P. R. Murray, E. J. L. McInnes, L. A. Jack, L. J. Yellowlees, N. Robertson, *Dalt. Trans.* **2008**, 3701–8.
- [19] E. C.-H. Kwok, M.-Y. Chan, K. M.-C. Wong, W. H. Lam, V. W.-W. Yam, *Chem. A Eur. J.* **2010**, *16*, 12244–54.
- [20] P. A. Scattergood, P. Jesus, H. Adams, M. Delor, I. V. Sazanovich, H. D. Burrows, C. Serpa, J. A. Weinstein, *Dalt. Trans.* **2015**, *44*, 11705–11716.
- [21] M. L. Muro, S. Diring, X. Wang, R. Ziessel, F. N. Castellano, *Inorg. Chem.* **2009**, *48*, 11533–11542.
- [22] E. O. Danilov, A. A. Rachford, S. Goeb, F. N. Castellano, *J. Phys. Chem. A* **2009**, *113*, 5763–8.
- [23] C. J. Adams, N. Fey, Z. A. Harrison, I. V. Sazanovich, M. Towrie, J. A. Weinstein, *Inorg. Chem.* **2008**, *47*, 8242–57.
- [24] J. Kang, X. Zhang, H. Zhou, X. Gai, T. Jia, L. Xu, J. Zhang, Y. Li, J. Ni, *Inorg. Chem.* **2016**, *55*, 10208–10217.
- [25] P. Ho, B. Zheng, D. Mark, W. Wong, D. W. Mccamant, R. Eisenberg, *Inorg. Chem.* **2016**, *55*, 8348–8358.
- [26] J. E. McGarrah, R. Eisenberg, *Inorg. Chem.* **2003**, *42*, 4355–65.
- [27] D. L. Mohler, D. Chen, V. Reddy, *Synthesis (Stuttg.)* **2002**, *6*, 745–748.
- [28] J. McMurray, *Organic Chemistry*, Thompson Books/Cole, New York, **2004**.
- [29] M. E. Hickey, P. P. Waymack, R. L. Van Etten, W. Lafayette, *Arch. Biochem. Biophys.*, **1976**, *172*, 439–448.
- [30] S. J. Kelly, D. E. Dardinger, L. G. Butler, *Biochemistry* **1975**, *14*, 4983–4988.
- [31] S. R. Houghton, J. Melton, J. Fortunak, D. H. Brown, C. N. Boddy, D. H. Brown Ripin, *Tetrahedron* **2010**, *66*, 8137–8144.
- [32] F. R. Hartley, Ed., *The Chemistry of Organophosphorus Compounds*, Wiley, **1990**.
- [33] S. D. Cummings, R. Eisenberg, *J. Am. Chem. Soc.* **1996**, *118*, 1949–1960.
- [34] F. Hua, S. Kinayyigit, A. A. Rachford, E. A. Shikhova, J. R. Cable,

FULL PAPER

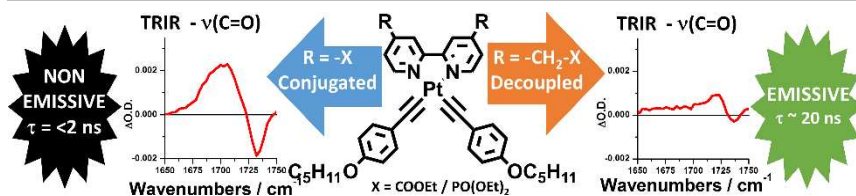
- C. J. Adams, K. Kirschbaum, A. A. Pinkerton, F. N. Castellano, S. Goeb, *Inorg. Chem.* **2007**, *46*, 8771–83.
- [35] C. J. Adams, S. L. James, X. Liu, P. R. Raithby, *Dalt. Trans.* **2000**, 63–67.
- [36] C. Whittle, J. A. Weinstein, M. W. George, K. S. Schanze, *Inorg. Chem.* **2001**, *40*, 4053–62.
- [37] I. E. Pomestchenko, C. R. Luman, M. Hissler, R. Ziessel, F. N. Castellano, *Inorg. Chem.* **2003**, *42*, 1394–6.
- [38] F. Hua, S. Kinayyigit, J. R. Cable, F. N. Castellano, *Inorg. Chem.* **2006**, *45*, 4304–6.
- [39] D. Beck, J. Brewer, J. Lee, D. McGraw, B. a. A. DeGraff, J. N. N. Demas, *Coord. Chem. Rev.* **2007**, *251*, 546–553.
- [40] E. S. Dodsworth, B. P. Lever, *Inorg. Chem.* **1990**, *29*, 499–503.
- [41] A. Marini, A. Mun, A. Biancardi, B. Mennucci, **2010**, 17128–17135.
- [42] W. Paw, S. D. Cummings, M. A. Mansour, W. B. Cennick, D. K. Geiger, D. Chemistry, N. Y, M. Adnan Mansour, W. B. Connick, R. Eisenberg, *Coord. Chem. Rev.* **1998**, *171*, 125–150.
- [43] J. Schneider, P. Du, P. Jarosz, T. Lazarides, X. Wang, W. W. Brennessel, R. Eisenberg, *Inorg. Chem.* **2009**, *48*, 1498–1506.
- [44] J. A. Zuleta, J. M. Bevilacqua, D. M. Proserpio, P. D. Harvey, R. E. J. R. Eisenberg, *Inorg. Chem.* **1992**, *1*, 2396–2404.
- [45] A. D. Laurent, D. Jacquemin, *Int. J. Quant. Chem.*, **2013**, *113*, 2019–2039.
- [46] C. Latouche, D. Skouteris, F. Palazzetti, V. Barone, *J. Chem. Theory Comput.*, **2015**, *11*, 3181–3289.
- [47] M. Hissler, W. B. Connick, D. K. Geiger, J. E. McGarrah, D. Lipa, R. J. Lachicotte, R. Eisenberg, *Inorg. Chem.* **2000**, *39*, 447–57.
- [48] K. Haskins-Glusac, I. Ghiviriga, K. A. Abboud, K. S. Schanze, *J. Phys. Chem. B* **2004**, *108*, 4969–4978.
- [49] J. V. Caspar, E. M. Kober, B. P. Sullivan, T. J. Meyer, *J. Am. Chem. Soc.* **1982**, *104*, 630–632.
- [50] R. M. Silverstein, F. X. Webster, *Spectrometric Identification of Organic Compounds*, Wiley, New York, **1998**.
- [51] E. A. Glik, S. Kinayyigit, K. L. Ronayne, M. Towrie, I. V. Sazanovich, J. A. Weinstein, F. N. Castellano, *Inorg. Chem.* **2008**, *47*, 6974–83.
- [52] I. V. Sazanovich, A. J. H. M. Meijer, J. A. Weinstein, *Phys. Chem. Chem. Phys.* **2014**, *16*, 25775–25788.
- [53] A. T. Yeh, C. V. Shank, J. K. McCusker, *Science* **2000**, *289*, 935–938.
- [54] A. Vlček, *Coord. Chem. Rev.* **2000**, *200–202*, 933–977.
- [55] R. M. Van Der Veen, A. Cannizzo, F. Van Mourik, A. Vlček, M. Chergui, *J. Am. Chem. Soc.* **2011**, *133*, 305–315.
- [56] T. Elsaesser, W. Kaiser, *Ann. Rev. Phys. Chem.* **1991**, *42*, 83–107.
- [57] B. S. Brunschwig, N. Sutin, *Coord. Chem. Rev.* **1999**, *187*, 233–254.
- [58] G. Ramakrishna, T. G. Iii, J. E. Rogers-haley, T. M. Cooper, D. G. Mclean, A. Urbas, T. Goodson III, *J. Phys. Chem. C* **2009**, *113*, 1060–1066.
- [59] F. N. Castellano, *Acc. Chem. Res.* **2015**, *48*, 828–839.
- [60] G. Greetham, P. Burgos, Q. Cao, I. Clark, P. Codd, R. Farrow, M. George, M. Kogimtzis, P. Matousek, A. W. Parker, et al., *Appl. Spectrosc.* **2010**, *64*, 1311–1319.
- [61] M. J. Frisch, G. W. Trucks, H. B. Schlegel, G. E. Scuseria, M. A. Robb, G. Cheeseman, J. R. Scalmani, V. Barone, B. Mennucci, G. A. Petersson, H. Nakatsuji, et al., **2010**.
- [62] R. C. Whaley, A. Petitet, J. J. Dongarra, *Parallel Comput.* **2001**, *27*, 3–35.
- [63] R. C. Whaley, A. Petitet, *Softw. Pract. Exp.* **2005**, *35*, 101–121.
- [64] A. D. Becke, *J. Chem. Phys.* **1993**, *98*, 5648.
- [65] R. Krishnan, J. S. Binkley, R. Seeger, J. A. Pople, *J. Chem. Phys.* **1980**, *72*, 650.
- [66] A. D. McLean, G. S. Chandler, *J. Chem. Phys.* **1980**, *72*, 5639.
- [67] D. Andrae, U. H. M. Dolg, H. Stoll, H. Preub, *Theor. Chim. Acta* **1990**, *77*, 123–141.
- [68] S. P. Foxon, C. Green, M. G. Walker, A. Wragg, H. Adams, J. A. Weinstein, S. C. Parker, A. J. H. M. Meijer, J. A. Thomas, *Inorg. Chem.* **2011**, *51*, 463–471.
- [69] I. V. Sazanovich, M. A. H. Alamiry, A. J. H. M. Meijer, M. Towrie, E. S. Davies, J. A. Weinstein, *Pure Appl. Chem.* **2013**, *85*, 1331–1348.
- [70] B. Mennucci, J. Tomasi, *J. Chem. Phys.* **1997**, *106*, 5151.
- [71] M. Cossi, V. Barone, B. Mennucci, J. Tomasi, *Chem. Phys. Lett.* **1998**, *286*, 253–260.
- [72] K. K. Irikura, R. D. Johnson, R. N. Kacker, *J. Phys. Chem. A* **2005**, *109*, 8430–7.
- [73] P. Sinha, S. E. Boesch, C. Gu, R. A. Wheeler, A. K. Wilson, *J. Phys. Chem. A* **2004**, *108*, 9213–9217.

FULL PAPER

Entry for the Table of Contents (Please choose one layout)

Layout 2:

FULL PAPER



Stuart A. Archer, Milan Delor, Theo Keane, Elizabeth Bevon, Alexander J. Auty, Dimitri Chekulaev, Igor V. Sazanovich, Michael Towrie, Anthony J. H. M. Meijer,* and Julia A. Weinstein*

Page No. – Page No.

Direct vs. Conjugated Attachment of electron withdrawing substituents on Pt(II) acetylides are studied using ultrafast time-resolved spectroscopy, examining the effect of decoupling the electron withdrawing group on the excited state.

Directly Coupled vs. Spectator Linkers on Diimine Pt(II) Acetylides – Change the Structure, Keep the Function?